

temperatures, and rapid pumping, we achieved 10^{-9} mbar. This allowed windowless operation between the storage ring, sample, and detector. Low temperature data collection also helped minimize radiation damage. For detection in this region, the most commonly used method is total electron yield, in which the emission of secondary photoelectrons is measured. The ~ 100 Å surface sensitivity and lack of specificity make this technique impractical for large molecules dilute in metal atoms such as metalloproteins. With a seven-element soft X-ray fluorescence array detector,¹⁷ we electronically resolved the Fe L fluorescence (705 eV) from the oxygen (525 eV), nitrogen (392 eV) and the carbon (277 eV) K fluorescence background. Since only a small fraction of absorption is due to Fe, fluorescence detection improves both the signal-to-noise and base-line stability.

L-edge data for oxidized (Fe^{3+}) and reduced (Fe^{2+}) rubredoxin are shown in Figure 1,¹⁶ together with results of theoretical calculations. The reduced L_3 edge has a maximum near 707.5 eV, a higher energy shoulder, and diffuse absorption features extending to 713 eV. The L_2 edge is broader and also tails to higher energy. Upon oxidation of the protein there is a ~ 800 meV increase in the main peak position, and the higher energy features become better separated.

To interpret these spectra, we used a theoretical simulation approach developed by Sawatzky, Thole, Fuggle, deGroot, and co-workers,^{6,18,19} based on earlier work by Cowan²⁰ and Butler.²¹ The calculation²² describes the transition from $3d^5$ (Fe^{3+}) and $3d^6$ (Fe^{2+}) to $2p3d^6$ and $2p3d^7$ (where $2p$ stands for the $2p$ core hole) in tetrahedral symmetry. The detailed structure at the L_3 ($2p_{3/2}$) and L_2 ($2p_{1/2}$) edges arises from final-state multiplet splittings from $3d-3d$ and $2p-3d$ Coulomb and exchange interactions, as well as ligand field d-orbital splittings. For simulating covalency effects on the experimental spectra, separation of the multiplet features can be controlled by an empirical reduction in the Slater integrals. Even for relatively ionic systems, electron correlation effects commonly require Slater integral reductions to 80% of theoretical values. In the rubredoxin simulations, the covalency of the S ligands is reflected in additional reductions (to $\sim 70\%$) required to model the data. Surprisingly, the covalency determined from the Slater integral reduction is similar for reduced and oxidized rubredoxin. Although one might expect that upon oxidation the extra hole would be mainly localized on the S neighbors, increasing the covalency, this might be counteracted by strong exchange stabilization of the high-spin $3d^5$ state.

(15) Blake, P. R.; Park, J.-B.; Bryant, F. O.; Aono, S.; Magnuson, J. K.; Eccleston, E.; Howard, J. B.; Summers, M. F.; Adams, M. W. W. *Biochemistry* **1991**, *30*, 10885-10895.

(16) The L-edge spectra were measured using AT&T Bell labs beam line U-4B¹ at the National Synchrotron Light Source, Brookhaven National Laboratory. A refocusing mirror produced a focused beam spot (1 mm \times 1.5 mm) enabling the sample to be mounted at glancing incidence (around 15° with respect to the incoming beam) without loss of incident X-ray intensity. Fluorescent X-rays from the protein samples were detected using a specially designed windowless seven-element germanium detector.¹⁷ The chamber was maintained at a vacuum of 2×10^{-9} mbar or better. After equilibration in a loadlock to 10^{-5} mbar, the samples were introduced into the main chamber and mounted on a precooled 10 K cold finger attached to a liquid helium flow cryostat. The L-edge spectra were collected as repetitive ~ 15 -min scans over a few hours. They were calibrated using the peak positions of the total electron yield spectra of MnF_2 and NiF_2 , with absorption maxima assigned as 640.0 and 852.7 eV, respectively.

(17) Cramer, S. P.; Tench, O.; Yocum, M.; Kraner, H.; Rogers, L.; Radeka, V.; Mullins, O.; Rescia, S. *X-ray absorption fine structure—Proceedings of the 6th International XAFS Conference*; Hasnain, S. S., Ed.; Ellis Horwood: Chichester, 1991; pp 640-645.

(18) Thole, B. T.; Cowan, R. D.; Sawatzky, G. A.; Fink, J.; Fuggle, J. C. *Phys. Rev. B* **1985**, *31*, 6856-6858.

(19) de Groot, F. M. F.; Fuggle, J. C.; Thole, B. T.; Sawatzky, G. A. *Phys. Rev. B* **1990**, *41*, 928-937.

(20) Cowan, R. D. *The Theory of Atomic Structure and Spectra*; University of California Press: Berkeley, 1981.

(21) Butler, P. H. *Point Group Symmetry, Applications, Methods, and Tables*; Plenum: New York, 1981.

(22) We used reduced Slater integrals F_{dd}^2 and F_{dd}^4 at 65% (d-d) and F_{pd}^2 , G_{pd}^1 , and G_{pd}^3 at 72.5% (p-d) for Fe^{3+} and 65% (all) for Fe^{2+} . To describe the different broadening processes present we broadened the spectra with a Lorentzian of 0.5 eV (L_3) and 1.0 eV (L_2) for the Fe^{3+} and 0.2 eV (L_3) and 0.8 eV (L_2) for the Fe^{2+} and convoluted with a Gaussian of 0.3 eV (Fe^{3+}) and 0.25 eV (Fe^{2+}).

Adjusting $10Dq$ in the simulations changes the spectral splittings and intensities, especially for the low-energy features below the strongest L_3 peak. The differences between purely atomic and ligand field calculations are illustrated in Figure 1. We found that $10Dq$ values of -0.75 ± 0.1 eV for Fe^{3+} and -0.60 ± 0.1 eV for Fe^{2+} gave reasonable simulations. Despite considerable optical work,²³⁻²⁶ $10Dq$ values for rubredoxin have not been reported. The X-ray parameters are similar to optical values for rubredoxin analogues $\text{Fe}^{\text{III}}[\text{S}(2,3,5,6\text{-Me}_4\text{C}_6\text{H}_4)]_4^-$ ($10Dq = -0.55$ eV)²⁶ and $\text{Fe}^{\text{II}}[\text{S}(2\text{-PhC}_6\text{H}_4)]_4^{2-}$ ($10Dq = -0.43$ eV).²⁷ Some caution must be used in comparing $10Dq$ values, because the XAS $10Dq$ value is determined by the $2p3d^{n+1}$ final states instead of the $3d^n$ multiplet states.

Certain discrepancies remain. There is additional intensity at the high-energy side of the L_3 edge (~ 712 eV); for Ni compounds this was shown to be a satellite structure.³ Although the experimental oxidized rubredoxin L_2 edge is broad and symmetric, the simulations gave an asymmetric double-peaked structure. Calculations assuming D_{2d} symmetry did not significantly improve the modeling. Although additional work is needed to fully explain the spectra, soft X-ray spectroscopy can be a valuable tool for bioinorganic studies.

Acknowledgment. This work was supported by the National Institutes of Health, Grant GM-44380 (to S.P.C.), and by LBL Exploratory Research Funds (to S.P.C.). National Science Foundation Grant DMB-88-05-255 (to M.W.W.A.) and support from the Netherlands Foundation for Chemical Research and the Committee for European Development of Science and Technology (to B.G.S.) are acknowledged. The National Synchrotron Light Source is funded by the Department of Energy, Office of Basic Energy Sciences.

(23) Bertrand, P.; Gayda, J.-P. *Biochim. Biophys. Acta* **1988**, *954*, 347-350.

(24) Bennett, D. E.; Johnson, M. K. *Biochim. Biophys. Acta* **1987**, *911*, 71-80.

(25) Eaton, W. A.; Lovenberg, W. In *Iron-Sulfur Proteins*; Academic Press: New York, 1973; Vol. II, pp 131-162.

(26) Gebhard, S. M.; Deaton, J. S.; Koch, S. A.; Millar, M.; Solomon, E. I. *J. Am. Chem. Soc.* **1990**, *112*, 2217-2231.

(27) Gebhard, S. M.; Koch, S. A.; Millar, M.; Devlin, F. J.; Stephens, P. J.; Solomon, E. I. *J. Am. Chem. Soc.* **1991**, *113*, 1640-1649.

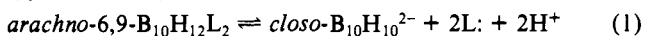
Electrophilic Reactions of Protonated *closo*- $\text{B}_{10}\text{H}_{10}^{2-}$ with Arenes, Alkane C-H Bonds, and Triflate Ion Forming Aryl, Alkyl, and Triflate *nido*-6-X- $\text{B}_{10}\text{H}_{13}$ Derivatives

M. Frederick Hawthorne,* Ipe J. Mavunkal, and Carolyn B. Knobler

Department of Chemistry and Biochemistry
University of California at Los Angeles
Los Angeles, California 90024

Received February 21, 1992

The preferred synthesis of *closo*- $\text{B}_{10}\text{H}_{10}^{2-}$ utilizes the loss of two skeletal electron pairs and two protons from *arachno*-6,9- $\text{B}_{10}\text{H}_{12}\text{L}_2$ where L = two-electron donor (eq 1).¹ The reverse process was later reported using HCl as the proton source and typically $(\text{C}_2\text{H}_5)_2\text{S}$ as the electron donor.²



We now report the facile two-electron reduction of *closo*- $\text{B}_{10}\text{H}_{10}^{2-}$ by reaction with benzene, cyclohexane, or triflate ion in the presence of triflic acid ($\text{CF}_3\text{SO}_3\text{H}$) forming the corre-

(1) (a) Hawthorne, M. F.; Pitochelli, A. R. *J. Am. Chem. Soc.* **1959**, *81*, 5519. (b) *Inorganic Syntheses*; Tyree, S. Y., Ed.; McGraw-Hill: New York, 1967; Vol. 9, p 16.

(2) Marshall, M. D.; Hunt, R. M.; Hefferman, G. T.; Adams, R. M.; Makhlof, J. M. *J. Am. Chem. Soc.* **1967**, *89*, 3361.

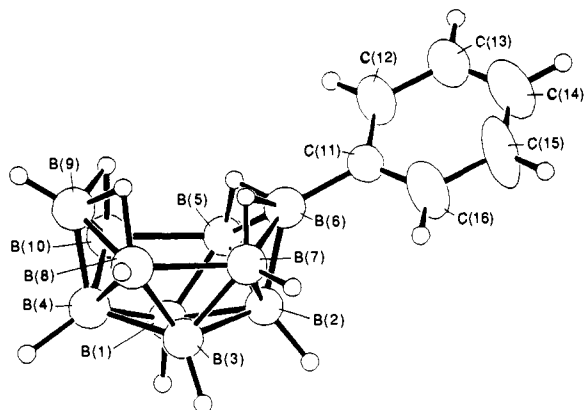


Figure 1. The molecular structure of **1** with thermal ellipsoids drawn at 50% probability. Selected interatomic distances (Å): B(6)–C(11), 1.569 (12); B(5)–B(10), 2.040 (14); B(7)–B(8), 1.957 (15). All the B–B distances are comparable with the B–B distances reported for $B_{10}H_{14}$.

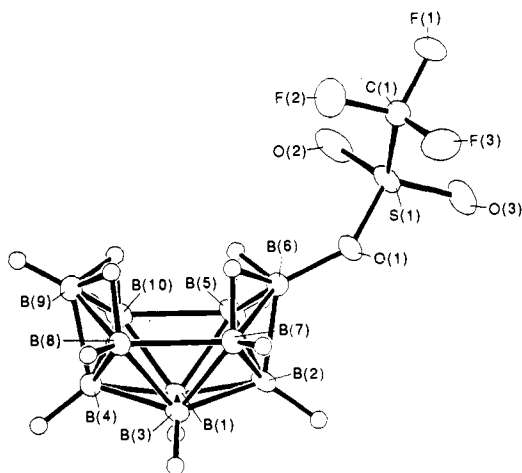


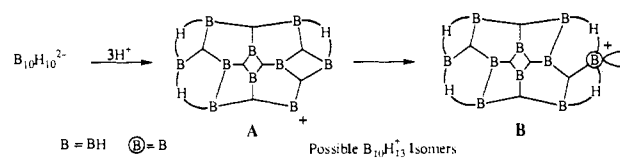
Figure 2. The molecular structure of **3** with thermal ellipsoids drawn at 50% probability. Selected interatomic distances (Å): B(5)–B(10), 1.982 (6); B(7)–B(8), 1.981 (6); B(6)–O(1), 1.433 (4); S(1)–O(1), 1.541 (2); S(1)–O(2), 1.410 (3); S(1)–O(3), 1.416 (3). All the B–B distances are comparable with the B–B distances reported for $B_{10}H_{14}$.

sponding *nido*-6-X- $B_{10}H_{13}$ species where X = phenyl, cyclohexyl, or triflate ($CF_3SO_3^-$).

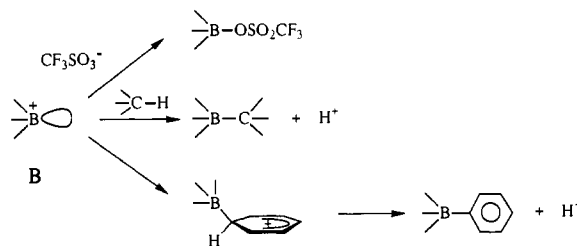
The reaction of a well-stirred suspension of $Cs_2B_{10}H_{10}$ in benzene at room temperature with 3 equiv of CF_3SO_3H rapidly produced CF_3SO_3Cs and *nido*-6-phenyl- $B_{10}H_{13}$, **1**, in 84% yield. An X-ray diffraction study established the structure of **1** (Figure 1),³ a previously reported compound.⁴ Substitution of cyclohexane

(3) Crystal data: $B_{10}H_{13}C_6$, orthorhombic, $P2_1ab$ (standard setting $Pca2_1$), $a = 10.9862$ (6) Å, $b = 10.8965$ (6) Å, $c = 21.875$ (1) Å, $V = 2619$ Å³, and $Z = 8$; $\mu_a = 2.8$ cm⁻¹, $D(\text{calcd}) = 1.01$ g cm⁻³, $T = 298$ K, $\alpha = 1.5418$ Å, graphite monochromator, colorless crystal, $0.025 \times 0.2 \times 0.5$ mm. A colorless platelet obtained from pentane solution was mounted on a fiber on a Syntex P1 diffractometer modified by Prof. C. E. Strouse of this department. Systematic absences were found for $hk0$ reflections, $k \neq 2n$, and for $h0l$ reflections, $h \neq 2n$. Unit cell parameters were determined from a least-squares fit of 28 accurately centered reflections ($18.1^\circ < 2\theta < 37.8^\circ$). Data were collected at 298 K in the θ - 2θ scan mode. Of the 1905 unique reflections measured, 1068 were considered observed, $I > 3\sigma(I)$, and were used in subsequent calculations. Data were corrected for Lorentz and polarization effects and for decay and extinction but not for absorption. Programs used in this work are included in the UCLA Crystallography Package. Atoms were located by use of direct methods (SHELX86). All carbon atoms were refined anisotropically. All other non-hydrogen atoms were refined isotropically. All phenyl H atoms were included in calculated positions as members of rigid C_6H_5 groups, C–C = 1.395 Å and C–H = 1.0 Å, angles = 120° . Boranyl H atoms were included in located positions. H atoms were assigned u values based approximately on the u value of the attached atom. Scattering factors for H were obtained from Stewart et al. (Stewart, R. F.; Davidson, E. R.; Simpson, W. T. *J. Chem. Phys.* **1965**, *42*, 3175) and for other atoms were taken from the following: *The International Tables for X-ray Crystallography*; Kynoch Press: Birmingham, England, 1974; Vol. IV. The larger peaks on a final difference electron density map were 0.1 e Å⁻³. The final discrepancy indices are $R = 0.078$, $R_w = 0.087$, GOF = 2.08.

Scheme I

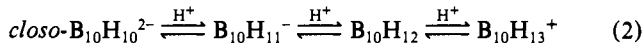


Scheme II



for benzene in this reaction produced an oil (10%), which was characterized as *nido*-6-cyclohexyl- $B_{10}H_{13}$,⁵ **2**, by NMR, MS, and oxidation with alkaline H_2O_2 ,⁶ followed by the identification of cyclohexanol using GLC/MS. The cyclohexane reaction was accompanied by the formation of polymeric substances and *nido*-6- CF_3SO_3 - $B_{10}H_{13}$, **3**, which was independently prepared by carrying out the above reaction in cyclopentane, separation from polymeric material by sublimation, and recrystallization from cyclopentane at -4 °C. The structure of **3** (Figure 2) was established by an X-ray diffraction study.⁷

In coordinating solvents, L, the $B_{10}H_{11}^-$ (or $B_{10}H_{11}L^-$) ion,⁸ and *arachno*-6,9- $B_{10}H_{12}L_2$ species² formed from $B_{10}H_{10}^{2-}$, HCl, and excess L (eq 1) were reported many years ago. The availability in noncoordinating solvents of a 22-electron borane electrophile of sufficient reactivity to affect electrophilic substitution of an arene or activation of an alkane C–H bond is unprecedented, and the reversible formation of a series of 22-electron borane species by successive protonation is suggested (eq 2). The regioselectivity



observed in these electrophilic hydrocarbon reactions as well as

(4) (a) Loffredo, R. E.; Drullinger, L. F.; Slater, J. A.; Turner, C. A.; Norman, A. D. *Inorg. Chem.* **1976**, *15*, 478. (b) Siedle, A. R.; McDowell, D.; Todd, L. J. *Inorg. Chem.* **1974**, *13*, 2735. (c) Hanousek, F.; Stibr, B.; Hermanek, S.; Plešek, J.; Vitek, A.; Harnda, F. *Collect. Czech. Chem. Commun.* **1972**, *37*, 3001.

(5) $B_{10}H_{13}(C_6H_{11})$ was previously prepared by the reaction of $B_{10}H_{13}MgX$ with cyclohexyl fluoride. Gallagher, J.; Siegel, B. *J. Am. Chem. Soc.* **1959**, *81*, 504.

(6) Brown, H. C.; Subba Rao, B. C. *J. Am. Chem. Soc.* **1956**, *78*, 5694.

(7) Crystal data: $B_{10}H_{13}SO_3CF_3$, orthorhombic $Pcab$ (standard setting $Pbca$), $a = 10.3745$ (9) Å, $b = 10.3764$ (10) Å, $c = 23.146$ (2) Å, $V = 2492$ Å³, and $Z = 8$; $\mu_a = 2.4$ cm⁻¹, $D(\text{calcd}) = 0.93$ g cm⁻³, $T = 156$ K, $\lambda = 0.7107$ Å, graphite monochromator, colorless cut parallelepiped specimen, $0.24 \times 0.27 \times 0.19$ mm. A crystal obtained from a cyclopentane solution was sealed in a capillary and placed on a Picker FACS-1 diffractometer modified by Prof. C. E. Strouse of this department. Systematic absences were found for $0kl$ reflections for which $l \neq 2n$, for $h0l$ reflections for which $h \neq 2n$, and for $hk0$ reflections for which $k \neq 2n$. Unit cell parameters were determined from a least-squares fit of 27 accurately centered reflections ($7.6 < 2\theta < 18.8^\circ$). Data were collected at 156 K in the θ - 2θ scan mode. Of the 3643 unique reflections measured, 1577 were considered observed ($I > 3\sigma(I)$) and were used in the subsequent structure analysis. Data were corrected for Lorentz and polarization effects and for secondary extinction but not for absorption. Programs used in this work are included in the UCLA Crystallography Package. Atoms were located by use of direct methods (SHELX86). All non-hydrogen atoms were refined with anisotropic parameters. Positions of H atoms were refined. H atoms were assigned an isotropic displacement value of 0.05 Å². Scattering factors for H were obtained from Stewart et al. (Stewart, R. F.; Davidson, E. R.; Simpson, W. T. *J. Chem. Phys.* **1965**, *42*, 3175) and for other atoms were taken from the following: *The International Tables for X-ray Crystallography*; Kynoch Press: Birmingham, England, 1974; Vol. IV. The maximum and minimum peaks on a final difference electron density map were 0.1 e Å⁻³. The final discrepancy indices are $R = 0.043$, $R_w = 0.050$, GOF = 1.47.

(8) (a) Wegner, P. A.; Adams, D. M.; Callabretta, F. J.; Spada, L. T.; Unger, R. G. *J. Am. Chem. Soc.* **1973**, *95*, 7513. (b) Wegner, P. A.; Unger, R. G.; Wiersema, R.; Hawthorne, M. F. Unpublished results, 1973.

the formation of the triflate derivative (vertex 6 in *nido*-B₁₀H₁₄) suggests that the arylation, alkylation, and triflation reactions all proceed from a common high-energy intermediate which is produced only in noncoordinating solvents. As shown in eq 2, the boranocation, B₁₀H₁₃⁺, is a presentable candidate for this intermediate.

The addition of three protons to the *closo*-B₁₀H₁₀²⁻ might produce an open B₁₀H₁₃⁺ cage having but 22 skeletal electrons, such as (A), which could rearrange to an isomer with 24 skeletal electrons (B) by conversion of an empty localized skeletal orbital to an empty terminal boron orbital by an internal hydride migration (Scheme I). The cationic B-6 of B then attacks available electron sources without great discrimination (Scheme II).

The proposed generation and reactions of a boranocation are without precedent, but the experimental results reported here fall into the same category and require an unusual explanation. Work continues with this fascinating chemistry.

Acknowledgment. This research was supported by Grant CHE-91-11437 from the National Science Foundation.

Supplementary Material Available: Tables of position and thermal parameters, bond lengths and angles, and crystallographic data for 1 and 3 (12 pages); listing of observed and calculated structure factors for 1 and 3 (15 pages). Ordering information is given on any current masthead page.

Observation of Fluorescence Emission from Solutions of C₆₀ and C₇₀ and Measurement of Their Excited-State Lifetimes

Dongho Kim* and Minyung Lee

*Spectroscopy Laboratory
Korea Research Institute of Standards and Science
Taedok Science Town, Taejeon 305-606, Korea*

Yung Doug Suh and Seong Keun Kim*

*Department of Chemistry
Seoul National University
Seoul 151-742, Korea*

Received January 27, 1992

Revised Manuscript Received February 19, 1992

Since the early stage of research on bulk C₆₀ and related fullerenes, much interest has been shown in the optical spectra of these species in an effort to elucidate the electronic structures and their implication in the chemistry and physics of the fullerene family. Absorption spectra of C₆₀ solutions in the UV-visible range were obtained by many groups¹⁻⁴ and show good agreement among them. A typical absorption spectrum shows a very weak absorption band between 430 and 620 nm, probably due to a forbidden transition, and a series of stronger absorption peaks at shorter wavelengths. The absorption spectrum of C₇₀ shows weak and broad absorption around 470 nm and further stronger absorption features at shorter wavelengths.²⁻⁴ However, no emission spectrum for C₆₀ in room temperature solution has been reported to date, although in low-temperature solids weak fluorescence has been observed.^{5,6} Things have been mostly similar in the case of C₇₀,⁷

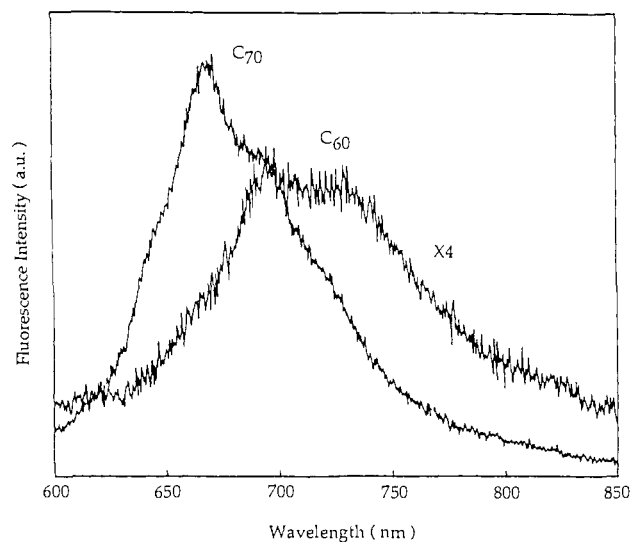


Figure 1. Fluorescence emission spectra of C₆₀ and C₇₀ in toluene at room temperature (excitation wavelength = 525 nm).

but room temperature fluorescence spectra from hexane and benzene solutions were reported to be observed as broad emission between 650 and 725 nm.⁷ The fluorescence was found to be very weak, with a quantum yield of about 8.5×10^{-4} . Transient absorption measurements of these fullerenes yielded indirect estimates for the lifetime of the excited singlet state C₆₀ as 1.2 ns⁸ or 0.65 ns,⁹ and that for C₇₀ as 0.67 ns.¹⁰ Lifetimes as short as 33 ps for C₆₀ and 0.11 ns for C₇₀ have also been suggested.¹¹

We report here the first observation of very weak fluorescence emission from highly purified samples of both C₆₀ and C₇₀ in toluene and in benzene at room temperature. The fullerenes were produced by the contact-arc method and purified by now-standard procedures.¹² FT-IR, Raman, and ¹³C NMR spectroscopy as well as HPLC and mass spectrometry were employed to identify the species. For C₆₀, the sample purity was estimated to be 99.5% or higher from mass spectrometric measurement. The purity of the C₇₀ sample was also very high, ca. 98%, and the only detectable impurity was C₆₀.

Figure 1 shows fluorescence emission spectra of C₆₀ and C₇₀ in toluene following excitation at 525 nm. The emission spectra were obtained on a SLM-Aminco spectrofluorometer. The concentration of C₆₀ in solution was 1×10^{-3} M. The C₇₀ solution was diluted to match the optical density of C₆₀ at the excitation wavelength. Emission from C₆₀ solution is broad but matches very well the 20 K luminescence spectrum of solid C₆₀ film deposited on CaF₂,⁵ and especially the luminescence spectrum of polycrystalline solid at 5 K.⁶ In the 20 K luminescence study, Whetten, Diederich, and co-workers observed 1420-cm⁻¹ spacings in their absorption spectrum. This was compared to the energy of one quantum of the totally symmetric (A_g) pentagonal pinch mode¹⁴ in the ground state, 1469 cm⁻¹, reduced by only 5% presumably due to a geometry similar to that of the ground state. In their emission spectra they also observed single vibronic structure with

(7) Arbogast, J. W.; Foote, C. S. *J. Am. Chem. Soc.* **1991**, *113*, 8886.

(8) Ebbesen, T. W.; Tanigaki, K.; Kuroshima, S. *Chem. Phys. Lett.* **1991**, *181*, 501.

(9) Sension, R. J.; Phillips, C. M.; Szarka, A. Z.; Romanow, W. J.; McGhie, A. R.; McCauley, J. P., Jr.; Smith, A. B., III; Hochstrasser, R. M. *J. Phys. Chem.* **1991**, *95*, 6075.

(10) Tanigaki, K.; Ebbesen, T. W.; Kuroshima, S. *Chem. Phys. Lett.* **1991**, *185*, 189.

(11) Wasielewski, M. R.; O'Neil, M. P.; Lykke, K. R.; Pellin, M. J.; Gruen, D. M. *J. Am. Chem. Soc.* **1991**, *113*, 2774.

(12) Parker, D. H.; Wurz, P.; Chatterjee, K.; Lykke, K. R.; Hunt, J. E.; Pellin, M. J.; Hemminger, J. C.; Gruen, D. M.; Stock, L. M. *J. Am. Chem. Soc.* **1991**, *113*, 7499.

(13) Whetten, R. L.; Alvarez, M. M.; Anz, S. J.; Schriver, K. E.; Beck, R. D.; Diederich, F. N.; Rubin, Y.; Ettl, R.; Foote, C. S.; Darmanyan, A. P.; Arbogast, J. W. *Mater. Res. Soc. Symp. Proc.* **1991**, *206*.

(14) Bethune, D. S.; Meijer, G.; Tang, W. C.; Rosen, H. J.; Golden, W. G.; Seki, H.; Brown, C. A.; de Vries, M. S. *Chem. Phys. Lett.* **1991**, *179*, 181.

(1) Krätschmer, W.; Lamb, L. D.; Fostiropoulos, K.; Huffman, D. R. *Nature* **1990**, *347*, 354.

(2) Ajie, H.; Alvarez, M. M.; Anz, S. J.; Beck, R. D.; Diederich, F.; Fostiropoulos, K.; Huffman, D. R.; Krätschmer, W.; Rubin, Y.; Schriver, K. E.; Sensharma, D.; Whetten, R. L. *J. Phys. Chem.* **1990**, *94*, 8630.

(3) Hare, J. P.; Kroto, H. W.; Taylor, R. *Chem. Phys. Lett.* **1991**, *177*, 394.

(4) Howard, J. B.; McKinnon, J. T.; Makarovskiy, Y.; Lafleur, A. L.; Johnson, M. E. *Nature* **1991**, *352*, 139.

(5) Reber, C.; Yee, L.; McKiernan, J.; Zink, J. I.; Williams, R. S.; Tong, W. M.; Ohlberg, D. A. A.; Whetten, R. L.; Diederich, F. *J. Phys. Chem.* **1991**, *95*, 2127.

(6) Sibley, S. P.; Argentine, S. M.; Francis, A. H. *Chem. Phys. Lett.* **1992**, *188*, 187.